INTERNATIONAL JOURNAL FOR NUMERICAL METHODS IN ENGINEERING, VOL. 30, 981–1011 (1990)

SPECIFICATIONS OF BOUNDARY CONDITIONS FOR REISSNER/MINDLIN PLATE BENDING FINITE ELEMENTS

BO HÄGGBLAD

Asea Brown Boveri Corporate Research, S-721 78 Västerås, Sweden

KLAUS-JÜRGEN BATHE

Massachusetts Institute of Technology, Cambridge, MA 02139, U.S.A.

SUMMARY

Plate bending finite elements based on the Reissner/Mindlin theory offer improved possibilities to pursue reliable finite element analyses. The physical behaviour near the boundary can be modelled in a realistic manner and inherent limitations in the Kirchhoff plate bending elements when modelling curved boundaries can easily be avoided. However, the boundary conditions used are crucial for the quality of the solution. We identify the part of the Reissner/Mindlin solution that controls the boundary layer and examine the behaviour near smooth edges and corners. The presence of boundary layers of different strengths for different sets of boundary conditions is noted. For a corner with soft simply supported edges the boundary layer removes the singular behaviour of Kirchhoff type from the stress resultants. We demonstrate the theoretical results by some numerical studies on simple plate structures which are discretized by an accurate, higher-order plate element. The results provide guidance in choosing efficient meshes and appropriate boundary conditions in finite element analyses.

1. INTRODUCTION

In finite element analysis, the early plate bending elements have usually been formulated using Kirchhoff plate theory. However, elements based on the refined Reissner/Mindlin plate theory are increasingly used in research and engineering practice, e.g. References 1–7. These elements are attractive, because they are of low order (only continuous interpolations are required) and can model both thin and moderately thick plate situations.

In this context it is important to recognize the differences to the Kirchhoff plate theory.[9] The Reissner/Mindlin plate theory is closer to a full 3-D description. It includes shear deformation effects, and on the edge of the plate three kinematic variables can be specified instead of only the transverse displacement and its normal derivative in the Kirchhoff theory. This makes it easy to avoid inherent limitations in the Kirchhoff plate bending elements (overconstraining effects and paradoxical results for polygonal domains) and the engineer can obtain much more reliable information about the stress state near supporting boundaries (in particular near corners). However, to achieve these improvements the appropriate boundary conditions must be imposed.

The main objective of this paper is to provide insight and guidance into how to choose meshes and boundary conditions when using Reissner/Mindlin plate theory based finite elements. The essential information is obtained by analysing the boundary layer behaviour near edges and corners. Special emphasis is focused on thin plate situations wehre the specification of the three boundary conditions for the Reissner/Mindlin plate may not be so obvious.

0029–5981/90/130981–31$15.50

Received 28 February 1989
Revised 15 January 1990

Questions of convergence (in abstract norms) of two-dimensional plate solutions to three-dimensional continuum solutions and the relationship between the Kirchhoff and the Reissner/Mindlin solutions have been studied by e.g. Ciarlet and Destuynder[8] and Bathe and Brezzi.[10] Important theoretical background results for this work can be found in the publications by Friedrichs and Dressler[11] and Reissner.[12,13] These authors show that the classical Kirchhoff solution may be viewed as a close approximation to the interior portion of the exact solution of the original three-dimensional problem, but the details of the edge-zone portion of the solution are not in general captured (Figure 1).

The Reissner/Mindlin theory provides a two-fold improvement over the Kirchhoff theory, namely

(i) a more accurate two-dimensional approximation to the three-dimensional edge-zone solution (that in general includes a boundary layer), and
(ii) an interior solution that includes shear deformation effects.

These improvements make it possible to specify realistic boundary conditions and obtain corrections for shear deformation effects which are of the same nature as the transverse shear correction in Timoshenko beams.

Considering the specifications of boundary conditions, Arnold and Falk have recently studied the boundary layers near smooth edges of a Reissner/Mindlin plate.[14,15] They use the direct approach with transverse displacements and rotations as primary unknowns and develop asymptotic expressions for these quantities in powers of the plate thickness. They also give rigorous bounds for the errors in the expansions. In this paper we use a different approach and give additional results. In our approach the deformation of the plate is represented by the transverse displacement of the mid-surface and the local twist of fibres originally perpendicular to the mid-surface. The transverse displacement is controlled by a biharmonic differential operator whereas the transverse twist is controlled by a singularly perturbed, elliptic differential operator which is responsible for the boundary layer (thin plate situations). The coupling between these two primary unknowns is obtained through the three boundary conditions.

We consider the behaviour of the edge-zone part of the Reissner/Mindlin solution for different choices of boundary conditions along a smooth edge far from corners. For an engineering important case (a plate with simply supported straight edges) we also investigate the theoretical behaviour of the Reissner/Mindlin solution *on* the edges when approaching a corner. We identify the non-analytic part of the transverse displacement that produces the singularity in the Kirchhoff moment tensor (obtuse corners). For a Reissner/Mindlin plate it is shown how the transverse twist removes this singularity and adjusts the moment tensor to zero across an edge zone. We also discuss how this affects the capability of modelling curved boundaries and the occurrence of possible paradoxical behaviour of the Reissner/Mindlin solution for regular

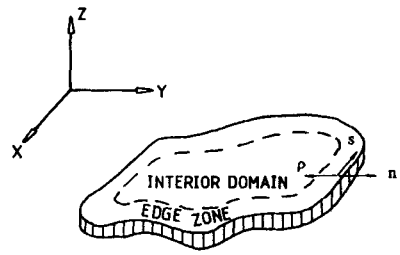

Figure 1. Edge zone of a Reissner/Mindlin plate

n-sided polygons (Babuska's paradox). Our objective in this paper is not to present a thorough mathematical analysis of the phenomena considered, but to present an engineering view of these phenomena. We present this view with sufficient rigour to firstly identify the phenomena and then to obtain good approximations of the stress quantities considered.

Using a high-order Reissner/Mindlin theory based plate element and a careful evaluation of boundary shearing forces, we demonstrate the theoretical results by finite element analyses of some simple plate structures. It is verified that the use of Reissner/Mindlin theory based plate elements in thin plate situations may prevent overconstraining (e.g. in the analysis of skew plates) if the boundary conditions are properly chosen.

2. THE REISSNER/MINDLIN THEORY

Using the notation and sign convention indicated in Figure 2, we summarize the basic continuum mechanics relations valid for most of the existing versions of the Reissner/Mindlin plate theory, irrespective of how they might have been motivated theoretically. Adopting the Reissner/Mindlin assumption of transverse inextensibility and constant transverse shear deformation through the thickness of the plate,[16,17] we obtain for $(x, y, z) \in A \times [-h/2, h/2]$ (A is the region in the xy-plane that is occupied by the mid-plane of the plate) a displacement field of the form

$$U(x, y, z) = z\Theta_x(x, y) \tag{1a}$$

$$V(x, y, z) = z\Theta_y(x, y) \tag{1b}$$

$$W(x, y, z) = w(x, y) \tag{1c}$$

where the three primary unknown fields are the transverse mid-plane displacement $w(x, y)$ and the rotations $\Theta_y(x, y)$ and $\Theta_x(x, y)$ of the normal to the mid-plane about the x- and y-axes, respectively.

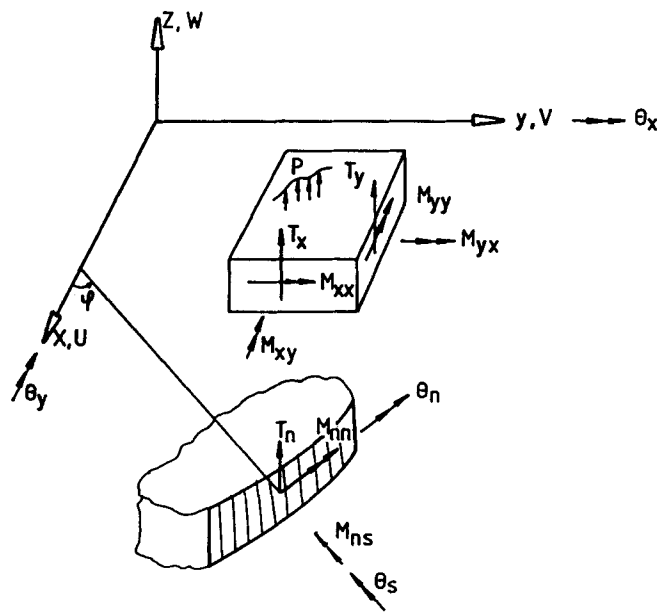

Figure 2. Notation and sign convention

The bending and twisting moments may be expressed in terms of rotations by the relations

$$M_{xx} = D_1 h^3 \left(\frac{\partial \Theta_x}{\partial x} + \nu \frac{\partial \Theta_y}{\partial y} \right) \tag{2a}$$

$$M_{yy} = D_1 h^3 \left(\nu \frac{\partial \Theta_x}{\partial x} + \frac{\partial \Theta_y}{\partial y} \right) \tag{2b}$$

and

$$M_{xy} = M_{yx} = D_1 h^3 \frac{1-\nu}{2} \left(\frac{\partial \Theta_y}{\partial x} + \frac{\partial \Theta_x}{\partial y} \right) \tag{2c}$$

with

$$D_1 = \frac{E}{12(1-\nu^2)}$$

where E and ν are the Young's modulus and Poisson's ratio, respectively. The shearing forces are given in terms of the transverse displacement $w(x, y)$ and the rotations $\Theta_x(x, y)$ and $\Theta_y(x, y)$ by the constitutive relations

$$T_x = D_2 h \left(\frac{\partial w}{\partial x} + \Theta_x \right) \tag{3a}$$

$$T_y = D_2 h \left(\frac{\partial w}{\partial y} + \Theta_y \right) \tag{3b}$$

where

$$D_2 = \frac{Ek}{2(1+\nu)}$$

with k as a shear correction factor.

An important quantity in the following investigation is the local transverse twist (Ω) which is obtained as

$$\Omega = \frac{\partial \omega}{\partial z} = \frac{1}{2} \left(\frac{\partial}{\partial x} \left(\frac{\partial V}{\partial z} \right) - \frac{\partial}{\partial y} \left(\frac{\partial U}{\partial z} \right) \right) = \frac{1}{2} \left(\frac{\partial \Theta_y}{\partial x} - \frac{\partial \Theta_x}{\partial y} \right) \tag{4}$$

where ω is the local rotation

$$\omega = \frac{1}{2} \left(\frac{\partial V}{\partial x} - \frac{\partial U}{\partial y} \right) \tag{5}$$

The local rotation in the mid-plane is always zero since in our bending theory the mid-plane cannot deform in its own plane. However, in planes parallel to the mid-plane the local rotation and the in-plane shear will in general be non-zero.

The equilibrium equations are

$$\frac{\partial M_{xx}}{\partial x} + \frac{\partial M_{xy}}{\partial y} = T_x \tag{6a}$$

$$\frac{\partial M_{xy}}{\partial x} + \frac{\partial M_{yy}}{\partial y} = T_y \tag{6b}$$

$$\frac{\partial T_x}{\partial x} + \frac{\partial T_y}{\partial y} = -p \tag{7}$$

Here $p = p(x, y)$ is the applied pressure load. The stress resultants M_{ns}, M_{nn} and T_n in Figure 2 are defined with respect to co-ordinate directions n and s, normal to and along the (boundary) curve. Relevant formulas valid in this natural system can be found in the Appendix.

In this study the applied load is chosen to depend on the plate thickness h in such a way that the limit problem ($h \to 0$) will produce solutions that are neither infinite nor zero. This is achieved by letting the prescribed pressure (p) and stress resultants be proportional to h^3:

$$p(x, y) = D_1 h^3 f(x, y) \tag{8}$$

$$T_x = D_1 h^3 \bar{T}_x \tag{9}$$

$$M_{xx} = D_1 h^3 \bar{M}_{xx} \tag{10}$$

etc.

where $\bar{T}_x$, $\bar{M}_{xx}$, etc. are scaled stress quantities. We also suppose that the fixed function $f(x, y)$ is smooth with well-defined derivatives of sufficiently high order. The interior part of the limit transverse displacement function will be the solution of a corresponding Kirchhoff problem and, as such, independent of the plate thickness, since the factor h^3 cancels out in the governing equation.

Observing that

$$D_1/D_2 = \frac{1}{6k(1-\nu)} \tag{11}$$

and using equations (2)–(3) and (6)–(8) we obtain the following fundamental relations:

$$\frac{\partial \bar{T}_x}{\partial x} + \frac{\partial \bar{T}_y}{\partial y} = -f \tag{12}$$

$$\Theta_x = -\frac{\partial w}{\partial x} + \frac{h^2}{6k(1-\nu)} \bar{T}_x \tag{13a}$$

$$\Theta_y = -\frac{\partial w}{\partial y} + \frac{h^2}{6k(1-\nu)} \bar{T}_y \tag{13b}$$

$$\bar{T}_x = -\frac{\partial}{\partial x}(\nabla^2 w) + \frac{h^2}{12k} \nabla^2 \bar{T}_x - \frac{h^2(1+\nu)}{12k(1-\nu)} \frac{\partial f}{\partial x} \tag{14a}$$

$$\bar{T}_y = -\frac{\partial}{\partial y}(\nabla^2 w) + \frac{h^2}{12k} \nabla^2 \bar{T}_y - \frac{h^2(1+\nu)}{12k(1-\nu)} \frac{\partial f}{\partial y} \tag{14b}$$

$$\bar{M}_{xx} = -\frac{\partial^2 w}{\partial x^2} - \nu \frac{\partial^2 w}{\partial y^2} + \frac{h^2}{6k(1-\nu)} \left(\frac{\partial \bar{T}_x}{\partial x} + \nu \frac{\partial \bar{T}_y}{\partial y} \right) \tag{15a}$$

$$\bar{M}_{yy} = -\nu \frac{\partial^2 w}{\partial x^2} - \frac{\partial^2 w}{\partial y^2} + \frac{h^2}{6k(1-\nu)} \left(\nu \frac{\partial \bar{T}_x}{\partial x} + \frac{\partial \bar{T}_y}{\partial y} \right) \tag{15b}$$

$$\bar{M}_{xy} = -(1-\nu) \frac{\partial^2 w}{\partial x \partial y} + \frac{h^2}{12k} \left(\frac{\partial \bar{T}_x}{\partial y} + \frac{\partial \bar{T}_y}{\partial x} \right) \tag{15c}$$

and

$$\nabla^4 w = f - \frac{h^2}{6k(1-\nu)} \nabla^2 f \tag{16}$$

Remark 1. It is clear that these expressions reduce to those of the Kirchhoff plate theory when $k \to \infty$, i.e. when we force the Reissner/Mindlin plate to become a Kirchhoff plate by a constitutive prescription. When $h \to 0$ the situation is much more complicated. In this paper we will concentrate on the *local* behaviour of the Reissner/Mindlin solution near edges and corners during such a limit process.

The structure of the transverse shearing forces is revealed if we rewrite the relations (14a) and (14b) in the form

$$\bar{T}_x + \frac{\partial}{\partial x}(\nabla^2 w) + \frac{h^2}{6k(1-\nu)}\frac{\partial f}{\partial x} = \frac{h^2}{12k}\left(\nabla^2 \bar{T}_x + \frac{\partial f}{\partial x}\right) \tag{17a}$$

and

$$\bar{T}_y + \frac{\partial}{\partial y}(\nabla^2 w) + \frac{h^2}{6k(1-\nu)}\frac{\partial f}{\partial y} = \frac{h^2}{12k}\left(\nabla^2 \bar{T}_y + \frac{\partial f}{\partial y}\right) \tag{17b}$$

Using equations (12) and (16) and the right hand side of equations (17a) and (17b) we obtain

$$\frac{\partial}{\partial x}\left(\nabla^2 \bar{T}_x + \frac{\partial f}{\partial x}\right) + \frac{\partial}{\partial y}\left(\nabla^2 \bar{T}_y + \frac{\partial f}{\partial y}\right) = 0 \tag{18}$$

Hence, the transverse shearing forces may be written

$$\bar{T}_x = -\frac{\partial}{\partial x}(\nabla^2 w) - \frac{h^2}{6k(1-\nu)}\frac{\partial f}{\partial x} + \frac{\partial \Psi}{\partial y} \tag{19a}$$

and

$$\bar{T}_y = -\frac{\partial}{\partial y}(\nabla^2 w) - \frac{h^2}{6k(1-\nu)}\frac{\partial f}{\partial y} - \frac{\partial \Psi}{\partial x} \tag{19b}$$

where Ψ is a stress function. Inserting equations (19a) and (19b) into equations (17a) and (17b) gives

$$\frac{\partial}{\partial y}\left(\Psi - \frac{h^2}{12k}\nabla^2 \Psi\right) = 0 \tag{20a}$$

and

$$\frac{\partial}{\partial x}\left(\Psi - \frac{h^2}{12k}\nabla^2 \Psi\right) = 0 \tag{20b}$$

Thus, Ψ is determined by an *elliptic* differential operator:

$$\frac{h^2}{12k}\nabla^2 \Psi - \Psi = \text{constant} = 0 \tag{21}$$

From equation (21) we conclude that for small h (or large k) the stress function exhibits a strong boundary layer behaviour within a distance of the order of $\sqrt{h^2/12k}$ from the boundary. Using the relations (21), (19a), (19b), (13a) and (13b) we obtain

$$\frac{12k}{h^2}\Psi = \nabla^2 \Psi = \frac{\partial \bar{T}_x}{\partial y} - \frac{\partial \bar{T}_y}{\partial x} = -\frac{6k(1-\nu)}{h^2}\left(\frac{\partial \Theta_y}{\partial x} - \frac{\partial \Theta_x}{\partial y}\right) = -\frac{12k}{h^2}(1-\nu)\Omega \tag{22}$$

which means that the stress function Ψ is essentially equal to the local transverse twist Ω:

$$\Psi = -(1-\nu)\Omega \tag{23}$$

In the following we prefer Ω to Ψ since Ω has a physical interpretation. Equations (16) and (21) are the two fundamental (decoupled) differential equations in the Reissner/Mindlin plate theory,[12] when it is formulated in terms of the transverse displacement w and the transverse twist Ω. The coupling between w and Ω is achieved through the boundary conditions. According to relation (16) the transverse displacement w is determined by the usual *biharmonic* differential operator, i.e. w has no boundary layer. However, it will contain shear deformation corrections of 'interior' type. The transverse twist *alone* governs the edge-zone behaviour of rotations and stress resultants. This may be seen more clearly by substituting equations (19a) and (19b) into the formulas (13)–(15). We use the natural co-ordinates (n, s) and limit ourselves to quantities that are employed to specify the most common boundary conditions (see Appendix). Thus, along any smooth (boundary) curve we have

$$\Theta_n = -\frac{\partial w}{\partial n} - \underline{\frac{h^2}{6k(1-\nu)}\frac{\partial}{\partial n}\left(\nabla^2 w + \frac{h^2 f}{6k(1-\nu)}\right)} - \underline{\underline{\frac{h^2}{6k}\frac{\partial \Omega}{\partial s}}} \tag{24a}$$

$$\Theta_s = -\frac{\partial w}{\partial s} - \underline{\frac{h^2}{6k(1-\nu)}\frac{\partial}{\partial s}\left(\nabla^2 w + \frac{h^2 f}{6k(1-\nu)}\right)} + \underline{\underline{\frac{h^2}{6k}\frac{\partial \Omega}{\partial n}}} \tag{24b}$$

$$\bar{T}_n = -\frac{\partial}{\partial n}\left(\nabla^2 w + \underline{\frac{h^2 f}{6k(1-\nu)}}\right) - \underline{\underline{(1-\nu)\frac{\partial \Omega}{\partial s}}} \tag{25a}$$

$$\bar{T}_s = -\frac{\partial}{\partial s}\left(\nabla^2 w + \underline{\frac{h^2 f}{6k(1-\nu)}}\right) + \underline{\underline{(1-\nu)\frac{\partial \Omega}{\partial n}}} \tag{25b}$$

$$\bar{M}_{nn} = -\frac{\partial^2 w}{\partial n^2} - \nu\left(\frac{\partial^2 w}{\partial s^2} + \dot{\varphi}\frac{\partial w}{\partial n}\right) - \underline{\frac{h^2 f}{6k(1-\nu)} - \frac{h^2}{6k}\left(\frac{\partial^2}{\partial s^2} + \dot{\varphi}\frac{\partial}{\partial n}\right)\left(\nabla^2 w + \frac{h^2 f}{6k(1-\nu)}\right)} - \underline{\underline{\frac{h^2}{6k}(1-\nu)\left(\frac{\partial^2 \Omega}{\partial s \partial n} - \dot{\varphi}\frac{\partial \Omega}{\partial s}\right)}} \tag{26a}$$

$$\bar{M}_{ss} = -\nu\frac{\partial^2 w}{\partial n^2} - \left(\frac{\partial^2 w}{\partial s^2} + \dot{\varphi}\frac{\partial w}{\partial n}\right) - \underline{\frac{\nu h^2 f}{6k(1-\nu)} - \frac{h^2}{6k}\left(\frac{\partial^2}{\partial s^2} + \dot{\varphi}\frac{\partial}{\partial n}\right)\left(\nabla^2 w + \frac{h^2 f}{6k(1-\nu)}\right)} + \underline{\underline{\frac{h^2}{6k}(1-\nu)\left(\frac{\partial^2 \Omega}{\partial s \partial n} - \dot{\varphi}\frac{\partial \Omega}{\partial s}\right)}} \tag{26b}$$

$$\bar{M}_{ns} = -(1-\nu)\frac{\partial^2 w}{\partial n \partial s} - \frac{h^2}{6k}\frac{\partial^2}{\partial n \partial s}\left(\nabla^2 w + \frac{h^2 f}{6k(1-\nu)}\right)$$

$$-\frac{h^2}{6k}(1-\nu)\left(\frac{\partial^2 \Omega}{\partial s^2} + \dot{\varphi}\frac{\partial \Omega}{\partial n}\right) + (1-\nu)\Omega \tag{26c}$$

Here, $\dot{\varphi} = \partial\varphi/\partial s$ denotes the curvature of the (boundary) curve. If the function f happens to be undefined on the boundary curve, we suppose that there exists a unique continuous extension of f that is defined on the boundary curve. We also assume that all (higher-order) differentiations can be performed without difficulties. Using the relations (A1), (A2) and (16) several alternative forms of the formulas (24)–(26) can be derived.

Remark 2. The replacement of w, Θ_x and Θ_y by w and Ω might look like a complication. However, in this way we obtain a formal decomposition of the solution in parts which we can compare with corresponding Kirchhoff expressions. In equations (24)–(26) the parts underlined with dashed lines correspond to boundary layer corrections that are predominant in the edge zone (when h is small). The transverse twist Ω is by definition different from zero only for truely two-dimensional problems, i.e. there is no boundary layer for one-dimensional problems (e.g. problems involving axisymmetry or Timoshenko beams). Specializing to one dimension we see that the parts underlined with solid lines correspond to the second-order corrections for the shear deformation in the Timoshenko beam theory.

Remark 3. Using space-theoretical concepts it is possible to prove convergence of the Reissner/Mindlin solution to a corresponding Kirchhoff solution in various Sobolev norms.[14,15] However, in an engineering context local (pointwise) convergence is of primary concern. We will see that there is a region of non-uniform convergence near the boundary, and local convergence to the Kirchhoff solution (measured by e.g. an absolute supremum norm) is not guaranteed on the boundary for all stress resultants.

3. EDGE-ZONE BEHAVIOUR

Letting $h \to 0$, we study the behaviour of the solution (w, Ω) of the sixth-order system

$$\nabla^4 w = f - \frac{h^2}{6k(1-\nu)}\nabla^2 f \tag{27a}$$

$$\frac{h^2}{12k}\nabla^2 \Omega - \Omega = 0 \tag{27b}$$

with appropriate boundary conditions specified for transverse displacement, rotations or stress resultants (expressed in terms of w and Ω according to the relations (24)–(26)). Considering equation (27b), it is clear that for decreasing h the transverse twist Ω plays an increasingly smaller role in the interior part of the plate. In thin plate situations Ω will be substantially different from zero only near the boundary and equation (27b) can be considered as a singular perturbation[18] of the equation

$$\Omega = 0 \tag{28}$$

Hence, in any *interior* domain the Reissner/Mindlin solution can be expected to converge for $h \to 0$ uniformly to a limit solution which is the corresponding Kirchhoff solution (see e.g.

References 14 and 15). However, as $h \to 0$ the boundary layer will shrink to zero width, ultimately including only the boundary curve.

In thin plate situations we want to look upon the Reissner/Mindlin solution (w, Ω) as a perturbed Kirchhoff solution (characterized by $w = w_0$ and $\Omega = \Omega_{00} \equiv 0$). Hence, the following asymptotic expansions in powers of h are assumed, see References 14 and 15

$$w = w_0 + hw_1 + h^2 w_2 + \ldots \tag{29a}$$

$$\Omega = \Omega_{00} + \chi(\Omega_0 + h\Omega_1 + h^2\Omega_2 + \ldots) \tag{29b}$$

where w_i are smooth interior expansion functions (independent of h). χ is a smooth cut-off function equal to one in the boundary layer zone and zero outside that region. Ω_i are boundary layer functions of the form

$$\Omega_i = \bar{\Omega}_i(\rho/h, s)\mathrm{e}^{-\kappa\rho/h} \tag{30}$$

where $\kappa = \sqrt{12k}$ and s is a co-ordinate along the boundary curve and ρ the distance from the point under consideration to the nearest point on the boundary (hence measured in the opposite direction of the external normal n to the boundary curve, see Figure 1). For a given h, $\bar{\Omega}_i(\rho/h, s)$ is a smooth function of s and the stretched variable ρ/h. The resulting 'one-dimensional' boundary layer function in equation (30) is strictly applicable to a smooth boundary curve with no corners. The functions $h^i\Omega_i$ represent boundary layers of different strengths (we use the power of h for the first non-vanishing term in the boundary layer expansion as a measure of the strength).

The expansion (29a) can be characterized as a regular perturbation expansion since w and all its derivatives converge uniformly ($h \to 0$) to its leading term, the Kirchhoff solution w_0 and its derivatives, in the *whole* domain A. The expansion (29b) is a singular perturbation expansion that adds corrections for the boundary layer to its leading term. In the limit ($h \to 0$) when the interior domain has expanded up to the boundary, the final remaining difference (if any) between the limit (Reissner/Mindlin) solution and the corresponding Kirchhoff solution should therefore be sought on the boundary curve.

Inserting the expansions (29) in the differential equations (27) and in the boundary conditions using the relations (24)–(26) and equating coefficients of equal powers of h gives a series of boundary value problems for w_i and Ω_i. These are solved in succession: $w_0 \to \Omega_0 \to w_1 \to \Omega_1 \to w_2 \to \Omega_2 \to \ldots$ in such a way that the boundary conditions are specified in terms of solution functions already determined by previous problems.

3.1. Simply supported edge

We start by considering a simply supported edge defined by the hard conditions

$$w = 0, \quad \Theta_s = 0, \quad \bar{M}_{nn} = 0 \tag{31}$$

Using the differential equations (27a, b) and the expressions (24b) and (26c) for the boundary conditions (remembering that $\partial w/\partial s = \partial^2 w/\partial s^2 = 0$ and that a differentiation of Ω_i in the normal direction picks out an inverse power of h) we can derive the boundary conditions for the series of boundary value problems for w_i and Ω_i. To simplify the algebra somewhat we use the expression (24b) together with a pair of new ones, derived from equations (24b), (26a) and (31):

$$(1 - \nu)\frac{\partial \Theta_s}{\partial s} + \bar{M}_{nn} = 0$$

$$\frac{\partial}{\partial s}\left((1 - \nu)\frac{\partial \Theta_s}{\partial s} + \bar{M}_{nn}\right) = 0$$

or

$$-\frac{\partial^2 w}{\partial n^2}-\frac{\partial^2 w}{\partial s^2}-\nu\dot{\varphi}\frac{\partial w}{\partial n}-\frac{h^2 f}{6k(1-\nu)}+\frac{h^2}{6k}\dot{\varphi}\frac{\partial}{\partial n}\left(\nabla^2 w+\frac{h^2 f}{6k(1-\nu)}\right)+\frac{h^2}{6k}(1-\nu)\dot{\varphi}\frac{\partial\Omega}{\partial s}=0 \tag{32a}$$

and

$$\frac{\partial}{\partial s}\left(\nabla^2 w+\frac{h^2 f}{6k(1-\nu)}\right)=\frac{\partial}{\partial s}\left((1-\nu)\dot{\varphi}\frac{\partial w}{\partial n}\right)+\frac{\partial}{\partial s}\left(\frac{h^2}{6k}\dot{\varphi}\frac{\partial}{\partial n}\left(\nabla^2 w+\frac{h^2 f}{6k(1-\nu)}\right)+\frac{h^2}{6k}(1-\nu)\dot{\varphi}\frac{\partial\Omega}{\partial s}\right) \tag{32b}$$

Equation (32a) gives the moment boundary conditions for w_i, and equation (24b) together with equation (32b) gives the Neumann boundary conditions for Ω_i. We obtain the following list of the first four pairs of boundary value problems (DE denotes differential equations and BC boundary conditions):

$$\text{DE:}\quad \nabla^4 w_0 = f \qquad \frac{h^2}{12k}\nabla^2\Omega_0-\Omega_0=0$$

$$\text{BC:}\quad w_0=0,\ \frac{\partial^2 w_0}{\partial n^2}+\dot{\varphi}\nu\frac{\partial w_0}{\partial n}=0 \qquad \frac{\partial(\Omega_0)}{\partial n}=0 \tag{33a}$$

$$\text{DE:}\quad \nabla^4 w_1=0 \qquad \frac{h^2}{12k}\nabla^2\Omega_1-\Omega_1=0$$

$$\text{BC:}\quad w_1=0,\ \frac{\partial^2 w_1}{\partial n^2}+\dot{\varphi}\nu\frac{\partial w_1}{\partial n}=0 \qquad \frac{\partial(h\Omega_1)}{\partial n}=\frac{\partial}{\partial s}\left(\dot{\varphi}\frac{\partial w_0}{\partial n}\right) \tag{33b}$$

$$\text{DE:}\quad \nabla^4 w_2=-\frac{1}{6k(1-\nu)}\nabla^2 f \qquad \frac{h^2}{12k}\nabla^2\Omega_2-\Omega_2=0$$

$$\text{BC:}\quad w_2=0,\ \frac{\partial^2 w_2}{\partial n^2}+\dot{\varphi}\nu\frac{\partial w_2}{\partial n} \qquad \frac{\partial(h\Omega_2)}{\partial n}=\frac{\partial}{\partial s}\left(\dot{\varphi}\frac{\partial w_1}{\partial n}\right)$$

$$=-\frac{f}{6k(1-\nu)}+\frac{\dot{\varphi}}{6k}\left(\frac{\partial(\nabla^2 w_0)}{\partial n}+(1-\nu)\frac{\partial\Omega_0}{\partial s}\right) \tag{33c}$$

$$\text{DE:}\quad \nabla^4 w_3=0 \qquad \frac{h^2}{12k}\nabla^2\Omega_3-\Omega_3=0$$

$$\text{BC:}\quad w_3=0,\ \frac{\partial^2 w_3}{\partial n^2}+\dot{\varphi}\nu\frac{\partial w_3}{\partial n} \qquad \frac{\partial(h\Omega_3)}{\partial n}=\frac{\partial}{\partial s}\left(\dot{\varphi}\frac{\partial w_2}{\partial n}\right)$$

$$=\frac{\dot{\varphi}}{6k}\left(\frac{\partial(\nabla^2 w_1)}{\partial n}+(1-\nu)\frac{\partial\Omega_1}{\partial s}\right) \qquad +\frac{1}{6k(1-\nu)}\frac{\partial}{\partial s}\left(\dot{\varphi}\frac{\partial(\nabla^2 w_0)}{\partial n}\right)+\frac{1}{6k}\frac{\partial}{\partial s}\left(\dot{\varphi}\frac{\partial\Omega_0}{\partial s}\right) \tag{33d}$$

From (33a) it follows that $\Omega_0 \equiv 0$. Hence, in general the resulting transverse twist is of the form $\Omega = h\Omega_1 + h^2\Omega_2 + \ldots$, i.e. a relatively 'weak' boundary layer. But from equations (24b) and (32b) it is also seen that the curvature controls the boundary layer. If the curvature $\dot{\varphi}$ is identically zero, Ω vanishes (all $\Omega_i \equiv 0$ in equations (33)) and there is no boundary layer effect at all.

If we change the condition $\Theta_s = 0$ to $\bar{M}_{ns} = 0$, i.e. we prescribe the more natural (soft) conditions

$$w = 0, \quad \bar{M}_{ns} = 0, \quad \bar{M}_{nn} = 0 \tag{34}$$

we do obtain a boundary layer even for zero curvature. Then equations (26a) and (26c) give the following new boundary value problems for w_i and Ω_i, respectively:

$$\begin{aligned}
&\text{DE:} \quad \nabla^4 w_0 = f && \frac{h^2}{12k}\nabla^2\Omega_0 - \Omega_0 = 0 \\
&\text{BC:} \quad w_0 = 0, \frac{\partial^2 w_0}{\partial n^2} + \dot{\varphi}\nu\frac{\partial w_0}{\partial n} = 0 && \Omega_0 = \frac{\partial^2 w_0}{\partial n \partial s} \not\equiv 0
\end{aligned} \tag{35a}$$

$$\begin{aligned}
&\text{DE:} \quad \nabla^4 w_1 = 0 && \frac{h^2}{12k}\nabla^2\Omega_1 - \Omega_1 = 0 \\
&\text{BC:} \quad w_1 = 0, \frac{\partial^2 w_1}{\partial n^2} + \dot{\varphi}\nu\frac{\partial w_1}{\partial n} && \Omega_1 = \frac{\partial^2 w_1}{\partial n \partial s} + \frac{\dot{\varphi}}{6k}\frac{\partial(h\Omega_0)}{\partial n} \\
&\qquad = -\frac{(1-\nu)}{6k}\frac{\partial^2(h\Omega_0)}{\partial n \partial s}
\end{aligned} \tag{35b}$$

$$\begin{aligned}
&\text{DE:} \quad \nabla^4 w_2 = -\frac{1}{6k(1-\nu)}\nabla^2 f && \frac{h^2}{12k}\nabla^2\Omega_2 - \Omega_2 = 0 \\
&\text{BC:} \quad w_2 = 0, \frac{\partial^2 w_2}{\partial n^2} + \dot{\varphi}\nu\frac{\partial w_2}{\partial n} && \Omega_2 = \frac{\partial^2 w_2}{\partial n \partial s} \\
&\qquad = -\frac{f}{6k(1-\nu)} + \frac{1}{6k}\left(\frac{\partial^2}{\partial s^2} + \dot{\varphi}\frac{\partial}{\partial n}\right)(\nabla^2 w_0) && \quad + \frac{1}{6k(1-\nu)}\frac{\partial^2(\nabla^2 w_0)}{\partial n \partial s} \\
&\qquad\quad - \frac{(1-\nu)}{6k}\left(\frac{\partial^2(h\Omega_1)}{\partial n \partial s} - \dot{\varphi}\frac{\partial\Omega_0}{\partial s}\right) && \quad + \frac{\dot{\varphi}}{6k}\frac{\partial(h\Omega_1)}{\partial n} + \frac{1}{6k}\frac{\partial^2\Omega_0}{\partial s^2}
\end{aligned} \tag{35c}$$

etc.

The physical interpretation of the application of these boundary conditions is that we introduce a transverse twist (local rotations in planes parallell to the mid-plane) near the boundary to make the in-plane shearing stresses (and hence the twisting moment) zero. The restulting transverse twist is of the form $\Omega = \Omega_0 + h\Omega_1 + h^2\Omega_2 + \ldots$, which gives a 'strong' boundary layer.

Using equations (29b) and (35a) and retaining only the first term we obtain following approximate expression for Ω close to the boundary:

$$\Omega(\rho, s) \approx \bar{\Omega}_0(\rho/h, s)\mathrm{e}^{-\kappa\rho/h} \tag{36}$$

where

$$\bar{\Omega}_0(\rho = 0, s) = \frac{\partial^2 w_0}{\partial n \partial s}(\rho = 0, s)$$

Inserting relation (36) in formulas (25a), (25b) and (26c) and neglecting the transverse shear correction term we can write down the following approximate expression for $\bar{T}_s$, $\bar{T}_n$ and $\bar{M}_{ns}$:

$$\bar{T}_n(s, \rho) = -\frac{\partial}{\partial n}(\nabla^2 w_0) - (1 - \nu)\frac{\partial}{\partial s}\left(\frac{\partial^2 w_0}{\partial n \partial s}\right) e^{-\kappa\rho/h} \tag{37a}$$

$$\bar{T}_s(s, \rho) = -\frac{\partial}{\partial s}(\nabla^2 w_0) + (1 - \nu)\frac{\partial^2 w_0}{\partial n \partial s}\frac{\kappa}{h} e^{-\kappa\rho/h} \tag{37b}$$

$$\bar{M}_{ns}(s, \rho) = -(1 - \nu)\frac{\partial^2 w_0}{\partial n \partial s} + (1 - \nu)\frac{\partial^2 w_0}{\partial n \partial s} e^{-\kappa\rho/h} \tag{37c}$$

where the derivatives of the Kirchhoff solution w_0 are evaluated *on the boundary* ($\rho = 0$). In thin plate situations these formulas often give satisfactory engineering accuracy (see Figures 3 and 4 and Reference 19).

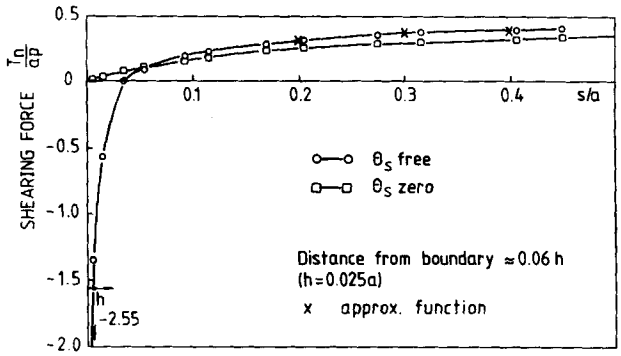

Figure 3. Shearing force distribution near the boundary

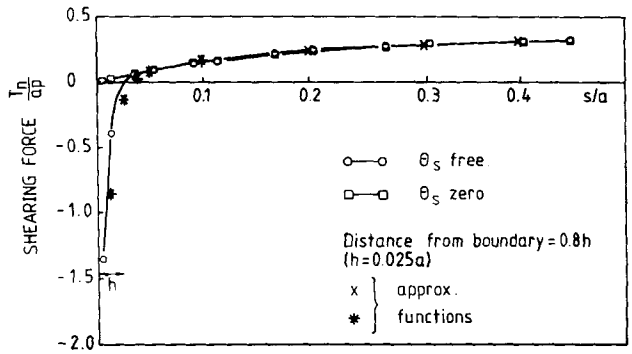

Figure 4. Shearing force distribution near the boundary

3.2. Clamped edge

In the same way we can consider a clamped edge defined either by

$$w = 0, \quad \Theta_s = 0, \quad \Theta_n = 0 \qquad \text{(hard conditions)} \tag{38a}$$

or

$$w = 0, \quad \bar{M}_{ns} = 0, \quad \Theta_n = 0 \qquad \text{(soft conditions)} \tag{38b}$$

The hard geometric conditions $\Theta_s = 0, \Theta_n = 0$ give, with equations (24a) and (24b), the following boundary value problems for w_i and Ω_i, respectively:

$$\begin{aligned}
&\text{DE:} \quad \nabla^4 w_0 = f && \frac{h^2}{12k}\nabla^2\Omega_0 - \Omega_0 = 0 \\
&\text{BC:} \quad w_0 = 0, \frac{\partial w_0}{\partial n} = 0 && \frac{\partial(\Omega_0)}{\partial n} = 0
\end{aligned} \tag{39a}$$

$$\begin{aligned}
&\text{DE:} \quad \nabla^4 w_1 = 0 && \frac{h^2}{12k}\nabla^2\Omega_1 - \Omega_1 = 0 \\
&\text{BC:} \quad w_1 = 0, \frac{\partial w_1}{\partial n} = 0 && \frac{\partial(h\Omega_1)}{\partial n} = \frac{1}{1-\nu}\frac{\partial(\nabla^2 w_0)}{\partial s} \not\equiv 0
\end{aligned} \tag{39b}$$

$$\begin{aligned}
&\text{DE:} \quad \nabla^4 w_2 = -\frac{1}{6k(1-\nu)}\nabla^2 f && \frac{h^2}{12k}\nabla^2\Omega_2 - \Omega_2 = 0 \\
&\text{BC:} \quad w_2 = 0, \frac{\partial w_2}{\partial n} && \frac{\partial(h\Omega_2)}{\partial n} = \frac{1}{1-\nu}\frac{\partial(\nabla^2 w_1)}{\partial s} \\
&\qquad = -\frac{1}{6k(1-\nu)}\frac{\partial(\nabla^2 w_0)}{\partial n} && \\
&\qquad -\frac{1}{6k}\frac{\partial\Omega_0}{\partial s} &&
\end{aligned} \tag{39c}$$

$$\begin{aligned}
&\text{DE:} \quad \nabla^4 w_3 = 0 && \frac{h^2}{12k}\nabla^2\Omega_3 - \Omega_3 = 0 \\
&\text{BC:} \quad w_3 = 0, \frac{\partial w_3}{\partial n} && \frac{\partial(h\Omega_3)}{\partial n} = \frac{1}{1-\nu}\frac{\partial(\nabla^2 w_2)}{\partial s} \\
&\qquad = -\frac{1}{6k(1-\nu)}\frac{\partial(\nabla^2 w_1)}{\partial n} && \qquad + \frac{1}{6k(1-\nu)^2}\frac{\partial f}{\partial s} \\
&\qquad -\frac{1}{6k}\frac{\partial\Omega_1}{\partial s} &&
\end{aligned} \tag{39d}$$

etc.

We see that the resulting transverse twist is of the form $\Omega = h\Omega_1 + h^2\Omega_2 + \ldots$, i.e. a 'weak' boundary layer. Here Ω is activated by the second-order transverse shear correction term in equation (24).

For the soft condition $\bar{M}_{ns} = 0$, equations (24a) and (26c) are combined to form a new relation

$$-(1-\nu)\frac{\partial\Theta_n}{\partial s} + \bar{M}_{ns} = 0$$

or

$$(1-\nu)\,\dot{\varphi}\frac{\partial w}{\partial s}+\frac{h^2}{6k}\,\dot{\varphi}\frac{\partial}{\partial s}\left(\nabla^2 w+\frac{h^2 f}{6k(1-\nu)}\right)-\frac{h^2}{6k}(1-\nu)\,\dot{\varphi}\frac{\partial\Omega}{\partial n}+(1-\nu)\Omega=0 \tag{40}$$

Using this relation, we obtain the following new boundary value problems for Ω_i:

$$\text{DE:}\quad \frac{h^2}{12k}\nabla^2\Omega_0-\Omega_0=0$$
$$\text{BC:}\quad \Omega_0=0 \tag{41a}$$

$$\text{DE:}\quad \frac{h^2}{12k}\nabla^2\Omega_1-\Omega_1=0$$
$$\text{BC:}\quad \Omega_1=\frac{\dot{\varphi}}{6k}\frac{\partial(h\Omega_0)}{\partial n} \tag{41b}$$

$$\text{DE:}\quad \frac{h^2}{12k}\nabla^2\Omega_2-\Omega_2=0$$
$$\text{BC:}\quad \Omega_2=\frac{\dot{\varphi}}{6k}\frac{\partial(h\Omega_1)}{\partial n}-\frac{\dot{\varphi}}{6k(1-\nu)}\frac{\partial(\nabla^2 w_0)}{\partial s} \tag{41c}$$

etc.

In general, the resulting transverse twist is of the form $\Omega = h^2\Omega_2 + \ldots$, i.e. a 'very weak' boundary layer. From equation (40) it follows that the curvature together with the second-order transverse shear correction term control the boundary layer. If the curvature $\dot{\varphi}$ is identically zero, Ω vanishes and there is no boundary layer effect.

3.3. *Free edge*

For the free edge, defined by $\bar{T}_n = 0$, $\bar{M}_{ns} = 0$ and $\bar{M}_{nn} = 0$ we use equations (25a), (26a) and (26c) and derive the following three relations

$$\left(\left(\frac{h^2}{6k}\dot{\varphi}\right)\bar{T}_n+\bar{M}_{nn}=0,\quad \bar{T}_n+\frac{\partial\bar{M}_{ns}}{\partial s}=0\quad\text{and}\quad\left(-\frac{h^2}{6k}\right)\frac{\partial\bar{T}_n}{\partial s}+\bar{M}_{ns}=0\right)$$

for the determination of the boundary conditions corresponding to moment, transverse force and transverse twist, respectively:

$$-\frac{\partial^2 w}{\partial n^2}-\nu\left(\frac{\partial^2 w}{\partial s^2}+\dot{\varphi}\frac{\partial w}{\partial n}\right)-\frac{h^2 f}{6k(1-\nu)}+\frac{h^2}{6k}\left(\frac{\partial^2}{\partial s^2}\right)\left(\nabla^2 w+\frac{h^2 f}{6k(1-\nu)}\right)$$
$$-\frac{h^2}{6k}(1-\nu)\left(\frac{\partial^2\Omega}{\partial s\partial n}\right)=0 \tag{42a}$$

$$-\frac{\partial}{\partial n}\left(\nabla^2 w+\frac{h^2 f}{6k(1-\nu)}\right)-(1-\nu)\frac{\partial}{\partial s}\left(\frac{\partial^2 w}{\partial n\partial s}\right)-\frac{h^2}{6k}\frac{\partial}{\partial s}\left(\frac{\partial^2}{\partial n\partial s}\left(\nabla^2 w+\frac{h^2 f}{6k(1-\nu)}\right)\right)$$
$$-\frac{h^2}{6k}(1-\nu)\frac{\partial}{\partial s}\left(\frac{\partial^2\Omega}{\partial s^2}+\dot{\varphi}\frac{\partial\Omega}{\partial n}\right)=0 \tag{42b}$$

$$-(1-\nu)\frac{\partial^2 w}{\partial n\partial s}-\frac{h^2}{6k}\dot{\varphi}\frac{\partial}{\partial s}\left(\nabla^2 w+\frac{h^2 f}{6k(1-\nu)}\right)-\frac{h^2}{6k}(1-\nu)\,\dot{\varphi}\frac{\partial\Omega}{\partial n}+(1-\nu)\Omega=0 \tag{42c}$$

The first three pairs of boundary value problems are:

$$\text{DE:}\quad \nabla^4 w_0 = 0 \qquad \frac{h^2}{12k}\nabla^2\Omega_0 - \Omega_0 = 0$$

$$\text{BC:}\quad \frac{\partial^2 w_0}{\partial n^2} + \nu\left(\frac{\partial^2 w_0}{\partial s^2} + \dot{\varphi}\frac{\partial w_0}{\partial n}\right) = 0 \qquad \Omega_0 = \frac{\partial^2 w_0}{\partial n \partial s} \not\equiv 0$$

$$\frac{\partial}{\partial n}(\nabla^2 w_0) + (1-\nu)\frac{\partial}{\partial s}\left(\frac{\partial^2 w_0}{\partial n \partial s}\right) = 0 \tag{43a}$$

$$\text{DE:}\quad \nabla^4 w_1 = 0 \qquad \frac{h^2}{12k}\nabla^2\Omega_2 - \Omega_2 = 0$$

$$\text{BC:}\quad \frac{\partial^2 w_1}{\partial n^2} + \nu\left(\frac{\partial^2 w_1}{\partial s^2} + \dot{\varphi}\frac{\partial w_1}{\partial n}\right) \qquad \Omega_1 = \frac{\partial^2 w_1}{\partial n \partial s} + \frac{\dot{\varphi}}{6k}\frac{\partial(h\Omega_0)}{\partial n}$$

$$= -\frac{1}{6k}(1-\nu)\left(\frac{\partial^2(h\Omega_0)}{\partial s \partial n}\right)$$

$$\frac{\partial}{\partial n}(\nabla^2 w_1) + (1-\nu)\frac{\partial}{\partial s}\left(\frac{\partial^2 w_1}{\partial n \partial s}\right)$$

$$= -\frac{1}{6k}(1-\nu)\frac{\partial}{\partial s}\left(\dot{\varphi}\frac{\partial(h\Omega_0)}{\partial n}\right) \tag{43b}$$

$$\text{DE:}\quad \nabla^4 w_2 = -\frac{1}{6k(1-\nu)}\nabla^2 f \qquad \frac{h^2}{12k}\nabla^2\Omega_2 - \Omega_2 = 0$$

$$\text{BC:}\quad \frac{\partial^2 w_2}{\partial n^2} + \nu\left(\frac{\partial^2 w_2}{\partial s^2} + \dot{\varphi}\frac{\partial w_2}{\partial n}\right) \qquad \Omega_2 = \frac{\partial^2 w_2}{\partial n \partial s} + \frac{\dot{\varphi}}{6k}\frac{\partial(h\Omega_1)}{\partial n}$$

$$= -\frac{f}{6k(1-\nu)} + \frac{1}{6k}\frac{\partial^2}{\partial s^2}(\nabla^2 w_0) \qquad + \frac{\dot{\varphi}}{6k(1-\nu)}\frac{\partial(\nabla^2 w_0)}{\partial s}$$

$$-\frac{1}{6k}(1-\nu)\left(\frac{\partial^2(h\Omega_1)}{\partial s \partial n}\right)$$

$$\frac{\partial}{\partial n}(\nabla^2 w_2) + (1-\nu)\frac{\partial}{\partial s}\left(\frac{\partial^2 w_2}{\partial n \partial s}\right)$$

$$= -\frac{1}{6k}\frac{\partial}{\partial s}\left(\frac{\partial^2}{\partial n \partial s}(\nabla^2 w_0)\right)$$

$$-\frac{1}{6k}(1-\nu)\frac{\partial}{\partial s}\left(\frac{\partial^2 \Omega_0}{\partial s^2}\right.$$

$$\left.+\dot{\varphi}\frac{\partial(h\Omega_1)}{\partial n}\right) - \frac{1}{6k}(1-\nu)\frac{\partial f}{\partial n} \tag{43c}$$

The resulting transverse twist is of the form $\Omega = \Omega_0 + h\Omega_1 + h^2\Omega_2 + \ldots$, i.e. we obtain a 'strong' boundary layer.

3.4. Resulting strengths of boundary layers

Considering the nature of the coupling between w and Ω in the boundary conditions for the Ω_i-problems we find that the strong boundary layers (for soft simply supported and free plates) are activated by the second-order (moment type) derivatives of w. The weak boundary layers for the clamped plate are activated by the second-order transverse shear correction terms, proportional to derivatives of $\nabla^2 w_i$ ($i = 0, 1, 2, 3, \ldots$) (i.e. the non-harmonic content of w_i). Also, one should note the role played by the curvature for the existence of the weakest boundary layers. The following list, valid for *homogeneous* boundary conditions along a smooth boundary curve of a Reissner/Mindlin plate, shows the resulting relative strengths of the different types of boundary layers (the h-power of the first non-vanishing boundary layer term is indicated in parentheses):

simply supported

$w = 0, \bar{M}_{ns} = 0, \bar{M}_{nn} = 0$ (soft conditions)

$\bar{T}_s(h^{-1}), \bar{T}_n(h^0), \bar{M}_{nn}(h^1), \bar{M}_{ss}(h^1), \bar{M}_{ns}(h^0), \Theta_s(h^1)$ and $\Theta_n(h^2)$

$w = 0, \Theta_s = 0, \bar{M}_{nn} = 0$ (hard conditions)

$\bar{T}_s(h^0), \bar{T}_n(h^1), \bar{M}_{nn}(h^2), \bar{M}_{ss}(h^2), \bar{M}_{ns}(h^1), \Theta_s(h^2)$ and $\Theta_n(h^3)$

(no boundary layers for zero curvature!)

clamped

$w = 0, \bar{M}_{ns} = 0, \Theta_n = 0$ (soft conditions)

$\bar{T}_s(h^1), \bar{T}_n(h^2), \bar{M}_{nn}(h^3), \bar{M}_{ss}(h^3), \bar{M}_{ns}(h^2), \Theta_s(h^3)$ and $\Theta_n(h^4)$

(no boundary layers for zero curvature!)

$w = 0, \Theta_s = 0, \Theta_n = 0$ (hard conditions)

$\bar{T}_s(h^0), \bar{T}_n(h^1), \bar{M}_{nn}(h^2), \bar{M}_{ss}(h^2), \bar{M}_{ns}(h^1), \Theta_s(h^2)$ and $\Theta_n(h^3)$

free

$\bar{T}_n = 0, \bar{M}_{ns} = 0, \bar{M}_{nn} = 0$

$\bar{T}_s(h^{-1}), \bar{T}_n(h^0), \bar{M}_{nn}(h^1), \bar{M}_{ss}(h^1), \bar{M}_{ns}(h^0), \Theta_s(h^1)$ and $\Theta_n(h^2)$

Remark 4. The clamped plate with soft conditions (surprisingly not with the hard conditions) has the weakest boundary layer of all cases and the solution, including all stress resultants, will converge to the corresponding Kirchhoff solution even on the boundaries. On the other hand, the simply supported plate with soft conditions and the free plate have the strongest boundary layers and here the convergence to the Kirchhoff solution is not guaranteed for the transverse forces and the twisting moment on the boundary curve.

In specifying boundary conditions in classical plate theory two of the three stress resultants are *contracted* to one, resulting in the two stress resultants

$$\tilde{M}_{nn} = -\frac{\partial^2 w_0}{\partial n^2} - \nu\left(\frac{\partial^2 w_0}{\partial s^2} + \dot{\varphi}\frac{\partial w_0}{\partial n}\right)$$

and

$$\tilde{R}_n = \tilde{T}_n + \frac{\partial \tilde{M}_{ns}}{\partial s} = -\frac{\partial}{\partial n}(\nabla^2 w_0) - (1-\nu)\frac{\partial}{\partial s}\left(\frac{\partial^2 w_0}{\partial n \partial s}\right)$$

where w_0 denotes the Kirchhoff displacement solution and $\tilde{R}_n$ the 'equivalent transverse shearing force'. If we use the Reissner/Mindlin solution w to form the same stress resultants we obtain

from equations (25a), (25b), (26a), (26c) and (29)

$$\bar{M}_{nn} = -\frac{\partial^2 w}{\partial n^2} - \nu\left(\frac{\partial^2 w}{\partial s^2} + \dot{\varphi}\frac{\partial w}{\partial n}\right) - \frac{h^2}{6k}\frac{\partial^2}{\partial n^2}\left(\nabla^2 w + \frac{h^2 f}{6k(1-\nu)}\right) - \frac{\nu h^2 f}{6k(1-\nu)} - \frac{h^2}{6k}(1-\nu)\frac{\partial^2 \Omega}{\partial n \partial s}$$

$$\to -\frac{\partial^2 w_0}{\partial n^2} - \nu\left(\frac{\partial^2 w_0}{\partial s^2} + \dot{\varphi}\frac{\partial w_0}{\partial n}\right) \tag{44}$$

and

$$\bar{R}_n = \bar{T}_n + \frac{\partial \bar{M}_{ns}}{\partial s} = -\frac{\partial}{\partial n}\left(\nabla^2 w + \frac{h^2 f}{6k(1-\nu)}\right) - (1-\nu)\frac{\partial}{\partial s}\left(\frac{\partial^2 w}{\partial n \partial s}\right) + \frac{h^2}{6k}\frac{\partial^2 \bar{T}_n}{\partial s^2} - \frac{h^2}{6k}\frac{\partial(\dot{\varphi}\bar{T}_s)}{\partial s}$$

$$\to -\frac{\partial}{\partial n}(\nabla^2 w_0) - (1-\nu)\frac{\partial}{\partial s}\left(\frac{\partial w_0}{\partial n \partial s}\right) \tag{45}$$

when $h \to 0$, except in points on the boundary where Ω, $\bar{T}_n$ or $\bar{T}_s$ have an unsmooth behaviour as functions of h (e.g. $(h^2/6k)\,(\partial^2 \bar{T}_n/\partial s^2)$ does not converge to zero as $h \to 0$). In these points (e.g. corners) formulas (44) and (45) suggest additional contributions that will be exemplified in the next section. Hence, even if $\bar{T}_n$ and $\bar{M}_{ns}$ do not converge separately to the corresponding Kirchhoff expressions the combination $\bar{R}_n = \bar{T}_n + \partial \bar{M}_{ns}/\partial s$ does. This is a natural consequence of force equilibrium of the shrinking boundary layer zone: the resulting total transverse stress on the inner part of the boundary layer, given by the Kirchhoff solution, must be in equilibrium with the resulting total transverse stress on the outer part (boundary curve), given by the Reissner/Mindlin solution.

Remark 5. The case with non-homogeneous boundary conditions can be treated in a similar way except that now the Kirchhoff component w_0 must satisfy the imposed non-homogeneous boundary conditions (or the corresponding Kirchhoff versions, $\partial w/\partial s \neq 0$, $\partial^2 w/\partial s^2 \neq 0$, etc.). As a result there will be a boundary layer behaviour even for straight edges with zero curvature.

4. BOUNDARY LAYERS NEAR A CORNER

In the preceding section we identified how a non-zero transverse twist adjusts the interior Kirchhoff solution to the boundary conditions of Reissner/Mindlin type within a narrow edge zone. However, in a corner some of the involved Kirchhoff stress resultants might be unlimited and if the corresponding Reissner/Mindlin quantities are prescribed to have finite values (e.g. zero) on the boundary curve, then the transverse twist removes the singularity *and* adjusts the solution to the prescribed boundary value within the edge zone. In the following we limit our discussion to the engineering important case of a corner (angle α, $0 < \alpha < \pi$) with simply supported straight edges. This case clearly demonstrates the smoothing effect of the transverse twist. For simplicity we also assume that the solution is symmetric with respect to the bisecting line (as in rhombic or regular polygonal plates) and that the loading is sufficiently smooth: $f(x, y)$ = constant uniformly over the plate. This simplified approach will enable us to interpret the results of the numerical experiments in Section 5.

Thus, we consider the solution of system (27) near a corner with simply supported edges. The transverse Reissner/Mindlin displacement contains, besides the smooth particular part, a biharmonic part that dominates near the corner. Using polar co-ordinates (r, ϕ), this part can be written (see e.g. Williams[20] or Morley[21] where the corresponding Kirchhoff solution is treated)

$$w = (a_1 + b_1 r^2) r^{\pi/\alpha} \sin(\phi\pi/\alpha) + \text{smoother terms} \tag{46}$$

(r = the distance from the corner, $0 \leqslant \phi \leqslant \alpha$, $0 < \alpha < \pi$)
which means that some stress resultants might become unlimited at the corner (see equations (24)–(26)). The second-order derivatives of w behave as $r^{\pi/\alpha - 2}$ and third-order derivatives seem to behave as $r^{\pi/\alpha - 3}$. However, it should be noted that the component in relation (46) that essentially controls the singular behaviour $(a_1 r^{\pi/\alpha} \sin(\phi\pi/\alpha))$ is *harmonic*, i.e. satisfies $\nabla^2 w = 0$, implying that the third-order derivatives are zero. Thus, the second-order shear correction terms in equations (24)–(26) that contain derivatives of $\nabla^2 w$ do not lower the regularity of the rotations and stress resultants but give a second-order contribution (proportional to h^2) for the biharmonic term $b_1 r^2 r^{\pi/\alpha} \sin(\phi\pi/\alpha)$. In our analysis we will assume that the co-ordinate axis for s is a straight line with the corner as origin ($s = 0$). The n-axis is perpendicular to the s-axis, pointing in the negative ϕ-direction (Figure 5). It is illustrative to list the Kirchhoff stress resultants and rotations for the dominating (harmonic) component:

$$\begin{aligned}
&\tilde{T}_s = 0 && \tilde{T}_n = 0\\
&\tilde{M}_{nn} \sim (1 - \nu)(\pi/\alpha)(\pi/\alpha - 1) r^{\pi/\alpha - 2} \sin(\phi\pi/\alpha)\\
&\tilde{M}_{ss} \sim -(1 - \nu)(\pi/\alpha)(\pi/\alpha - 1) r^{\pi/\alpha - 2} \sin(\phi\pi/\alpha)\\
&\tilde{M}_{ns} \sim (1 - \nu)(\pi/\alpha)(\pi/\alpha - 1) r^{\pi/\alpha - 2} \cos(\phi\pi/\alpha)\\
&\tilde{\Theta}_s \sim -(\pi/\alpha) r^{\pi/\alpha - 1} \sin(\phi\pi/\alpha) && \tilde{\Theta}_n \sim (\pi/\alpha) r^{\pi/\alpha - 1} \cos(\phi\pi/\alpha)
\end{aligned} \tag{47}$$

Hence, for the Kirchhoff plate the moment tensor $(\tilde{M}_{nn}, \tilde{M}_{ns}, \tilde{M}_{ns})$ is different from zero at the corner and has a singularity there when $\alpha > \pi/2$. The harmonic component is 'supported' only by moments (no transverse shearing forces at the boundaries). However, if we impose soft simply

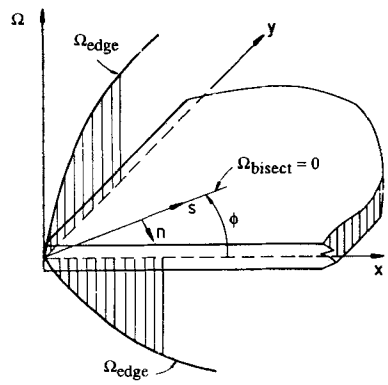

Figure 5. Transverse twist at a corner of a simply supported plate

supported boundary conditions for a Reissner/Mindlin plate the moment tensor is forced to take the value zero at the corner ($\bar{M}_{nn} = \bar{M}_{ss} = \bar{M}_{ns} = 0$) and will approach zero within a boundary layer in a direction from the interior domain of the plate. This means that restrictions are imposed on the derivatives of the transverse twist Ω in the formulas (24)–(26) such that they contain singularities that 'neutralize' the singularities in the derivatives of the transverse displacement w. In the following we study this interaction between the transverse twist and w along the straight edge when approaching the corner. It should also be noted that the physcial interpretation of Ω shows directly that along certain lines (curves) towards the corner its behaviour may be exceptional. Consider e.g. the line $x = y$ in a square plate (Figure 5), along which (due to symmetry) Ω and its directional derivatives are zero.

4.1. The transverse twist along an edge

The soft boundary condition $\bar{M}_{ns} = 0$ gives the following differential equation for Ω on a straight edge (equation (26c)) through the corner,

$$-\frac{h^2}{6k}\left(\frac{\partial^2 \Omega}{\partial s^2}\right) + \Omega = \frac{\partial^2 w}{\partial n \partial s} + \frac{h^2}{6k(1-\nu)}\frac{\partial^2}{\partial n \partial s}\left(\nabla^2 w + \frac{h^2 f}{6k(1-\nu)}\right) \tag{48a}$$

or

$$-(h_0)^2 \frac{\partial^2 \Omega}{\partial s^2} + \Omega = F(s) \tag{48b}$$

where we have introduced the characteristic 'width' h_0 of the boundary layer *on* the edge near the corner, defined by

$$(h_0)^2 = \frac{h^2}{6k} \tag{49}$$

(note that $h_0 \neq \sqrt{h^2/12k}$ which is the 'width' applicable to the normal direction of an edge far from a corner) and the notation

$$F(s) = \frac{\partial^2 w}{\partial n \partial s} + \frac{h^2}{6k(1-\nu)}\frac{\partial^2}{\partial n \partial s}\left(\nabla^2 w + \frac{h^2 f}{6k(1-\nu)}\right) \tag{50}$$

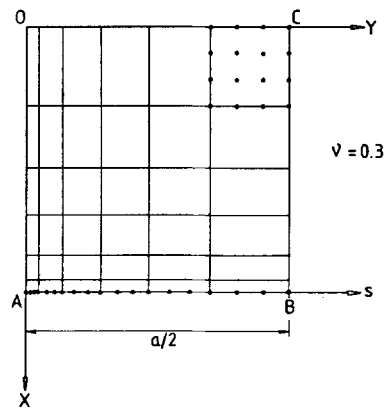

Figure 6. FE-model for a square plate

Strictly, F is also dependent on Ω via w. However, in thin plate situations w is almost equal to the Kirchhoff solution w_0 everywhere in the plate so this dependency can be neglected. The solution of equations (48) can be written on the general form

$$\Omega(s) = \left(\Omega(0) + \int_0^s F(t)\sinh\left(\frac{t}{h_0}\right)\frac{\mathrm{d}t}{h_0}\right)\frac{\sinh\left(\dfrac{b-s}{h_0}\right)}{\sinh\left(\dfrac{b}{h_0}\right)}$$

$$+\left(\Omega(b) + \int_s^b F(t)\sinh\left(\frac{b-t}{h_0}\right)\frac{\mathrm{d}t}{h_0}\right)\frac{\sinh\left(\dfrac{s}{h_0}\right)}{\sinh\left(\dfrac{b}{h_0}\right)} \tag{51}$$

$\Omega(0)$ and $\Omega(b)$ are boundary values that in general depend on h. b is typically taken greater than $5h_0$.

A usable approximation is obtained if we introduce exponentials and rearrange terms (assuming that $\mathrm{e}^{(s-b)/h_0} \ll 1$). Thus for small s

$$\Omega(s) \approx \Omega(0)\mathrm{e}^{-s/h_0} + I_1(b)\sinh\left(\frac{s}{h_0}\right) + I_2(s) \tag{52}$$

and

$$\frac{\partial\Omega(s)}{\partial s} \approx \frac{1}{h_0}\left(-\Omega(0)\mathrm{e}^{-s/h_0} + I_1(b)\cosh\left(\frac{s}{h_0}\right) - I_3(s)\right) \tag{53}$$

where

$$I_1(b) = \int_0^b F(t)\mathrm{e}^{-t/h_0}\frac{\mathrm{d}t}{h_0}, \qquad I_2(s) = \int_0^s F(t)\sinh\left(\frac{t-s}{h_0}\right)\frac{\mathrm{d}t}{h_0}$$

and

$$I_3(s) = \int_0^s F(t)\cosh\left(\frac{t-s}{h_0}\right)\frac{\mathrm{d}t}{h_0} \tag{54}$$

The interaction between the possible singularities of $F(t)$ for $t = 0$ and the boundary layer is contained in the integrals $I_1(b)$, $I_2(s)$ and $I_3(s)$.

4.2. A general corner

In the general case, for a corner with an angle α (π/α not equal to an integer), we can write for the dominating (non-analytic) biharmonic component on the edge

$$F(s) = \frac{\partial^2 w}{\partial n\partial s} + \frac{h^2}{6k(1-\nu)}\frac{\partial^2}{\partial n\partial s}(\nabla^2 w)$$

$$\approx -\frac{\pi}{\alpha}\left(\frac{\pi}{\alpha}-1\right)\left(a_1 + b_1\frac{4h^2}{6k(1-\nu)}\left(\frac{\pi}{\alpha}+1\right)\right)s^{\pi/\alpha-2}\cos(\phi\pi/\alpha) \sim -\frac{\pi}{\alpha}\left(\frac{\pi}{\alpha}-1\right)s^{\pi/\alpha-2}$$

Since $\Omega = 0$ along a symmetry line through the corner, we obtain $\Omega(0) = 0$. Thus

$$\Omega(s) \approx I_1(b)\sinh\left(\frac{s}{h_0}\right) + I_2(s)$$

$$\sim -h_0^{\pi/\alpha-2}\left(\Gamma\left(\frac{\pi}{\alpha}+1\right)-\left(\frac{s}{h_0}\right)^{\pi/\alpha-1}\right)\sinh(s/h_0) \tag{55}$$

and

$$\frac{\partial\Omega(s)}{\partial s}\approx\frac{1}{h_0}\left(I_1(b)\cosh\left(\frac{s}{h_0}\right)-I_3(s)\right)$$
$$\sim -h_0^{\pi/\alpha-3}\left(\Gamma\left(\frac{\pi}{\alpha}+1\right)-\left(\frac{s}{h_0}\right)^{\pi/\alpha-1}\right)\cosh(s/h_0)+h_0^{\pi/\alpha-3}\left(\frac{\pi}{\alpha}-1\right)\left(\frac{s}{h_0}\right)^{\pi/\alpha-1} \tag{56}$$

where

$$I_1(b)=-\frac{\pi}{\alpha}\left(\frac{\pi}{\alpha}-1\right)\int_0^b t^{\pi/\alpha-2}e^{-t/h_0}\frac{dt}{h_0}\approx -h_0^{\pi/\alpha-2}\Gamma\left(\frac{\pi}{\alpha}+1\right)$$

(Γ denotes the gamma function),

$$I_2(s)=-\frac{\pi}{\alpha}\left(\frac{\pi}{\alpha}-1\right)\int_0^s t^{\pi/\alpha-2}\sinh\left(\frac{t-s}{h_0}\right)\frac{dt}{h_0}$$
$$\approx\frac{\pi}{\alpha}\left(\frac{\pi}{\alpha}-1\right)\sinh\left(\frac{s}{h_0}\right)\int_0^s t^{\pi/\alpha-2}\left(1-\frac{t}{s}\right)\frac{dt}{h_0}$$
$$=h_0^{\pi/\alpha-2}\left(\frac{s}{h_0}\right)^{\pi/\alpha-1}\sinh(s/h_0)$$

and

$$I_3(s)=-\frac{\pi}{\alpha}\left(\frac{\pi}{\alpha}-1\right)\int_0^s t^{\pi/\alpha-2}\cosh\left(\frac{t-s}{h_0}\right)\frac{dt}{h_0}$$
$$\approx -\frac{\pi}{\alpha}\left(\frac{\pi}{\alpha}-1\right)\int_0^s t^{\pi/\alpha-2}\left(\frac{t}{s}+\left(1-\frac{t}{s}\right)\cosh\left(\frac{s}{h_0}\right)\right)\frac{dt}{h_0}$$
$$=-h_0^{\pi/\alpha-2}\left(\frac{s}{h_0}\right)^{\pi/\alpha-1}\cosh(s/h_0)-\left(\frac{\pi}{\alpha}-1\right)h_0^{\pi/\alpha-2}\left(\frac{s}{h_0}\right)^{\pi/\alpha-1}$$

We note that the expression for $\Omega(s)$ contains non-analytic components ($\pi/\alpha \neq$ an integer) that neutralize the singularity in the twisting moment of the dominating biharmonic component, $(a_1 + b_1 r^2)r^{\pi/\alpha}\sin(\phi\pi/\alpha)$.

Remark 6. Equation (56) indicates that $\partial\Omega(s)/\partial s$ (and $\bar{T}_n$) will pass through zero close to the corner for small h_0. A formal equation for the zero passage is obtained from equation (56):

$$s/h_0=\left(\frac{\Gamma\left(\frac{\pi}{\alpha}+1\right)\cosh(s/h_0)}{\pi/\alpha-1+\cosh(s/h_0)}\right)^{1/(\pi/\alpha-1)} \tag{57}$$

which can be solved iteratively for s/h_0. s_{zero}/h_0 decreases slowly from 1·3 (for $\alpha=\pi/2$) to 0·7 (for $\alpha\Rightarrow\pi$). Since our approach is based on the assumption that $s^{\pi/\alpha-2}$ *dominates* the solution near the corner the formula (57) is expected to be applicable when $\alpha>\pi/2$. Since the derivative in equation (56) (and hence the transverse shearing force) has a very large slope near the corner for $\pi/2<\alpha<\pi$, the location of the zero passage may be used as a measure of the steepness of the

boundary layer. In any case, it should be an important parameter to consider when choosing a finite element mesh that will resolve the boundary layer behaviour. It is also clear that the value at the corner of the transverse shearing force corresponding to the dominating harmonic component determines if the boundary layer will be observable or not. From equation (56) we obtain

$$\bar{T}_n(0) = (1 - \nu)\frac{\partial \Omega(0)}{\partial s} \sim h_0^{\pi/\alpha - 3}\,\Gamma\left(\frac{\pi}{\alpha} + 1\right) \approx h_0^{\pi/\alpha - 3}\,\frac{\alpha}{\pi} \tag{58}$$

Hence for $\alpha > \pi/3$ a boundary layer should eventually appear if the plate thickness is decreased sufficiently. The applicability of formulas (57) and (58) is checked in numerical experiments (Section 5). Based on equations (57) and (58) the results for a corner with simply supported edges (soft conditions) can be summarized as follows. For $\pi/3 < \alpha < \pi$ the transverse shearing forces will have an observable boundary layer that passes zero close to the corner and the slope at the corner will be infinite if $\pi/2 < \alpha < \pi$. For obtuse angles the boundary layer becomes 'steeper' for increasing angles ('steepness' measured by the inverse of the distance from the corner to the point of zero). The bending moments will approach zero within an edge zone in the interior of the angle field with an increasingly steeper slope as α increases (the underlying Kirchhoff singularity becomes more severe).

Remark 7. For a simply supported, regular n-sided polygonal Kirchhoff plate, that is inscribed in a circle, there is a paradoxical behaviour as n increases and the polygon approaches the circle (Babuska's paradox[22]). Since the twisting moment cannot be specified separately in the Kirchhoff theory, the moment tensor will be non-zero (and, as we have seen, even singular) on the boundary of the polygon and the limit configuration will not be moment free on the boundary. For the Reissner/Mindlin plate the moment tensor becomes zero (across the edge zone) in every point of the polygonal boundary curve. The interior part of the solution approaches a rotationally symmetric state that is supported on the inner part of the edge zone by a system of stress resultants that is in equilibrium with the moment free boundary forces. Since this is valid for every value of n it is also valid for the limit configuration, where the transverse twist has approached zero throughout the plate (rotational symmetry).

Remark 8. It is easily seen that for a hard simply supported corner there is no boundary layer and the solution will be of Kirchhoff type with corner singularities and only a second-order shear correction improvement. Possible Kirchhoff singularities can only be removed if a boundary layer exists.

Remark 9. From the formulas (24), (40) and (42c) it follows that there will be no boundary layer *on* the edge towards the corner for the other types of homogeneous boundary conditions. The pure edge type boundary layers will occur near corner under the same conditions as stated in Section 3.

4.3. The right-angle corner

For a soft simply supported corner with a right angle ($\alpha = \pi/2$), we can use a constant function ($s^{\pi/\alpha - 2} = s^0$) as a first approximation of $F(s)$ near the corner. Here we choose

$$F(s) = F_0 = \left.\frac{\partial^2 w_0}{\partial n \partial s}\right|_{\text{corner}} = \frac{\partial^2 w_0}{\partial n \partial s}(s = 0)$$

in the formulas (52) and (53) (w_0 is the Kirchhoff solution). Thus

$$\Omega(s) \approx F_0 + (\Omega(0) - F_0)\frac{\sinh\left(\frac{b-s}{h_0}\right)}{\sinh\left(\frac{b}{h_0}\right)} \approx F_0 + (\Omega(0) - F_0)e^{-s/h_0}$$

$$= F_0(1 - e^{-s/h_0}) \tag{59}$$

and

$$\frac{\partial\Omega(s)}{\partial s} \approx -\frac{1}{h_0}(\Omega(0) - F_0)\frac{\cosh\left(\frac{b-s}{h_0}\right)}{\sinh\left(\frac{b}{h_0}\right)} \approx -\frac{1}{h_0}(\Omega(0) - F_0)e^{-s/h_0}$$

$$= \frac{F_0}{h_0}e^{-s/h_0} \tag{60}$$

Here we have utilized that $\Omega = 0$ in the corner, see Figure 5. From equation (25a) and the differential equation (48) we obtain on the edge *far from the corner*

$$\bar{T}_n = -\frac{\partial}{\partial n}\left(\nabla^2 w + \frac{h^2 f}{6k(1-\nu)}\right) - (1-\nu)\frac{\partial\Omega}{\partial s} \approx -\frac{\partial}{\partial n}\left(\nabla^2 w_0 + \frac{h^2 f}{6k(1-\nu)}\right)$$

$$-(1-\nu)\frac{\partial}{\partial s}\left(\frac{\partial^2 w_0}{\partial n\partial s}\right) \tag{61}$$

and *near the corner*

$$\bar{T}_n \approx -\frac{\partial}{\partial n}\left(\nabla^2 w + \frac{h^2 f}{6k(1-\nu)}\right) - (1-\nu)\frac{\partial F}{\partial s} - (1-\nu)\frac{h^2}{6k}\left(\frac{\partial^3\Omega}{\partial s^3}\right)$$

$$\approx -\frac{\partial}{\partial n}\left(\nabla^2 w_0 + \frac{h^2 f}{6k(1-\nu)}\right) - (1-\nu)\frac{\partial}{\partial s}\left(\frac{\partial^2 w_0}{\partial n\partial s}\right) - (1-\nu)\frac{F_0}{h_0}e^{-s/h_0}$$

$$\approx -(1-\nu)\frac{F_0}{h_0}e^{-s/h_0} \tag{62}$$

From the results contained in equations (61) and (62), we can conclude (as a consequence of force equilibrium of the edge zone) that in the limit $h_0 \to 0$, *the transverse boundary force distribution will approach a force distribution that is predicted on the basis of the contracted Kirchhoff boundary relations (including the concentrated forces)*. Thus, the (conventional) equivalent transverse shearing force distribution according to Kirchhoff can be thought of as a limit distribution for physically well-behaved Reissner/Mindlin force distributions when the plate thickness h is decreased, see also Remark 4. In the limit the quantity $D_1 h^3 \bar{T}_n(0)h_0$ represents a concentrated force of magnitude

$$D_1 h^3 \int_0^b \bar{T}_n \, dt \approx -D_1 h^3 \int_0^b (1-\nu)\frac{F_0}{h_0}e^{-t/h_0} \, dt$$

$$= -D_1 h^3 (1-\nu)\frac{\partial^2 w_0}{\partial n\partial s}\bigg|_{\text{corner}} \approx D_1 h^3 \bar{T}_n(0)h_0 \tag{63}$$

However, it should be observed that, for a plate with given finite thickness h, this limit distribution gives no reliable information about the stress state (including transverse shear stresses) around the corner. The applicability of formula (63) is checked in a numerical experiment (see Figure 7 and Table I). Of course, the moment tensor on the boundary will *not* converge to the corresponding Kirchhoff quantity. If we substitute in equation (62) more accurate Kirchhoff approximations such as[9]

$$F(s) = F_0 \cos(\pi s/a) \tag{64}$$

(a is the side-length, see Figure 6) and

$$-\frac{\partial}{\partial n}\left(\nabla^2 w_0 + \frac{h^2 f}{6k(1-\nu)}\right) \approx \frac{4fa}{\pi^2}\left(0{\cdot}917\sin(\pi s/a) + \frac{1}{9}\sin(3\pi s/a) + \frac{1}{25}\sin(5\pi s/a) + \frac{1}{49}\sin(7\pi s/a)\right) \tag{65}$$

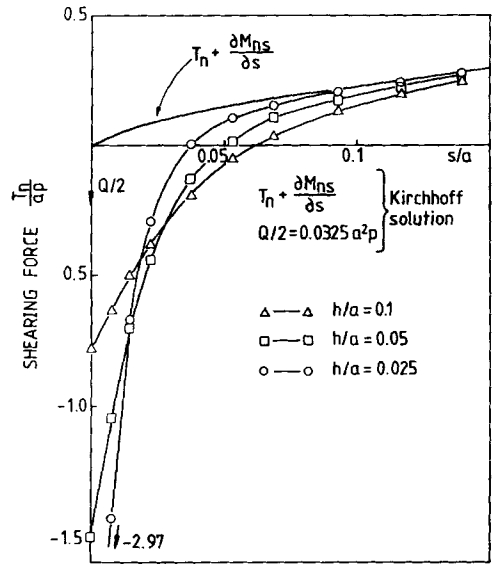

Figure 7. Shearing force distribution along AB

Table I

h/a		0·1	0·05	0·025
h_0/a		0·0447	0·0224	0·0112
$\frac{T_n(0)}{ap}$	(Figure 7)	− 0·77	− 1·5	− 2·97
$\frac{h_0}{a}\frac{T_n(0)}{ap}$	(equation (63))	− 0·0344	− 0·0335	− 0·0332

we obtain the expression

$$\frac{\bar{T}_n}{fa} \approx \frac{4}{\pi^2}\left(0{\cdot}917\sin(\pi s/a) + \frac{1}{9}\sin(3\pi s/a) + \frac{1}{25}\sin(5\pi s/a) + \frac{1}{49}\sin(7\pi s/a)\right)$$
$$+ 0{\cdot}0325\left(\pi\sin(\pi s/a) - \frac{a}{h_0}e^{-s/h_0}\right) \tag{66}$$

(here $(1-\nu)F_0$ is given the 'Kirchhoff' value $0{\cdot}0325fa^2$) which reproduces the behaviour of $\bar{T}_n$ near the corner very accurately (especially for thin plates, see Figure 8). A characteristic feature of the formula (66) is that it predicts that $\bar{T}_n$ passes zero increasingly closer to the corner when the plate becomes thinner.

5. NUMERICAL EXPERIMENTS

We demonstrate the theoretical results by some numerical experiments with simply supported plates with corner angles ranging from $\alpha = 30°$ to $\alpha = 150°$. In the finite element calculations we use the accurate 16-node plate element available in ADINA.[24]

Figure 6 shows a finite element model of a quarter of a simply supported square plate subjected to uniform pressure p (in the negative z-direction). From the boundary nodal point reaction forces along the edge AB a virtual work equivalent transverse shearing force distribution was computed. The shearing force is assumed to vary as a third-order (Lagrange) polynomial along each element side forming the edge AB.

Figure 9 shows the calculated transverse shearing force distribution along AB when the normal rotation is prescribed to zero ($\Theta_s = 0$) on the boundary. Since the values for the two thickness/length ratios coincide, the solution can be considered to have effectively converged to the thin plate limit. The figure indicates that the finite element model fails to describe the tendency of a simply supported plate to rise at the corners. The reaction forces at the corners are computed to

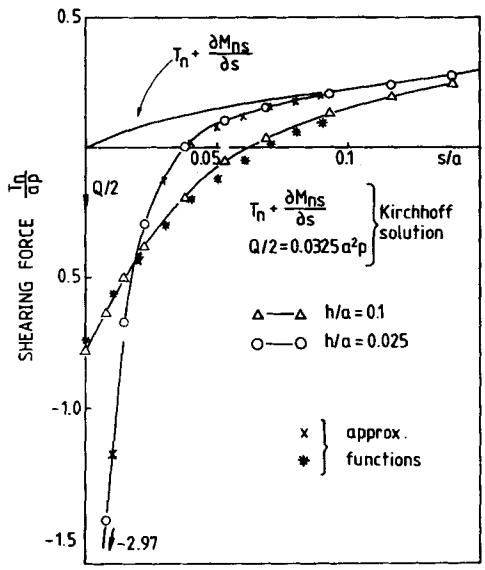

Figure 8. Shearing force distribution along AB obtained by approximate functions

be zero and the shearing force distribution coincides very accurately with a theoretical curve that is obtained by disregarding the twisting moment contribution in the equivalent Kirchhoff shearing force. That part is taken up as moment reactions at the boundary and Figure 10 shows that this distribution is in good agreement with the thin plate theory prediction (M_{ns}). Thus, all boundary layer effects have been filtered out by this choice of boundary conditions. If the normal rotation Θ_s is left free ($M_{ns} = 0$ in the finite element model) we obtain the results depicted in Figure 7.

According to equation (46) $\partial^2 w/\partial n \partial s$ is approaching a constant value in the corner and the 'Kirchhoff contribution' to the shearing force distribution is approaching zero. But the relations (62) and (66) indicate that a boundary layer is anticipated in the Reissner/Mindlin shear force distribution. In Figure 7 a 'natural' shearing force distribution is obtained. For decreasing h it converges towards the theoretical equivalent Kirchhoff solution in the interior and at some distance from the corner. In Figure 8 the approximative function values are computed with expression (66). Good agreement with the finite element results can be noted for thin plates. Using the calculated solution in Figure 7 we obtain the results in Table I.

According to Kirchhoff theory[9] the concentrated force at the corner has the value 0·0325 $a^2 p$. In Table I we have used $k = 5/6$.

Considering the uncertainties in the choice of k, etc., the table indicates that the shearing force distribution converges towards a distribution with concentrated forces of a magnitude that is

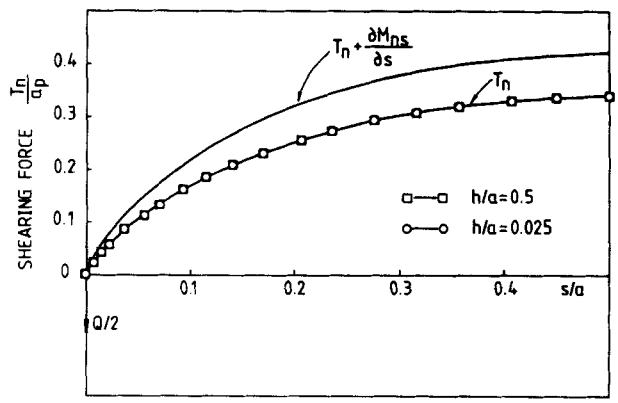

Figure 9. Shearing force distribution along AB

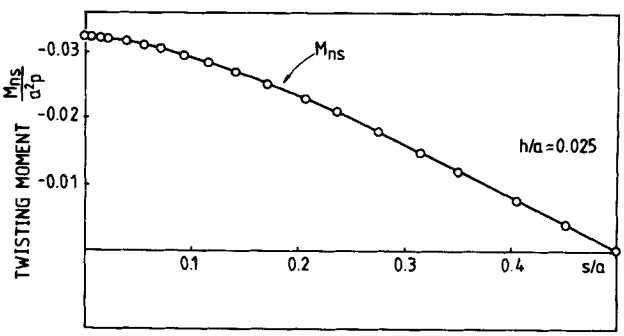

Figure 10. Twisting moment distribution along AB

predicted on the basis of the contracted (equivalent) boundary conditions in the Kirchhoff theory. Figures 3 and 4 show the boundary layer behaviour of the Reissner/Mindlin shearing force distribution. Figure 3 shows the shearing force distribution (T_n) in the row of Gauss points next to the boundary AB (distance = 0·06h). The curve –○– represents the case with Θ_s free and the curve –□– the case with Θ_s fixed (= 0). The change of the shearing force distribution from values on the boundary (Figure 7) to those at the distance 0·06h (Figure 3) is reproduced by the expression $e^{-\kappa\rho/h}$, where ρ is a co-ordinate normal to the boundary (see equation (37a)). In Figure 4 the same quantities are shown for a distance of 0·8h from the boundary. Here, except near the corner, the shearing force distributions already almost coincide. Also, the boundary layer is already of the pure 'edge-type' $(1/h)\, e^{-\kappa s/h}$ near $s = 0$ (see equation (37b) with $s \to n$ and $\rho \to s$, $\bar{T}_n$ along a cutting surface is equal to $\bar{T}_s$ for the adjacent perpendicular boundary surface). In Figures 3 and 4 the approximative function values are computed with equations (37a) and (37b), respectively. Thus, on the whole Figures 3, 4 and 7 confirm the boundary layer descriptions given by equations (37) and (66) with different decay lengths for 'pure' edges and corners.

We also discuss briefly some results for skew plates (uniform pressure p in positive z-direction, $h/a = 0{\cdot}025$) and apply the formulas (57)–(58). By leaving the normal rotation, Θ_s, free along the edge OB of the rhombic plate in Figure 11 ($\pi/\alpha = 6/5$, $\pi/\alpha = 6$) we obtain the transverse shearing force along OB shown in Figure 12 and the bending moment distributions along OA shown in Figure 13. From equation (58) we obtain $\bar{T}_n(0) \sim h_0^3$ in corner B and $\bar{T}_n(0) \sim h_0^{-9/5}$ in corner O and hence an observable boundary layer is not expected in corner B but in corner O, where the trend to infinity of the 'Kirchhoff contribution' is abruptly broken by the boundary layer. The formula (57) gives 0·009a for the location of the zero value near corner O. The moment

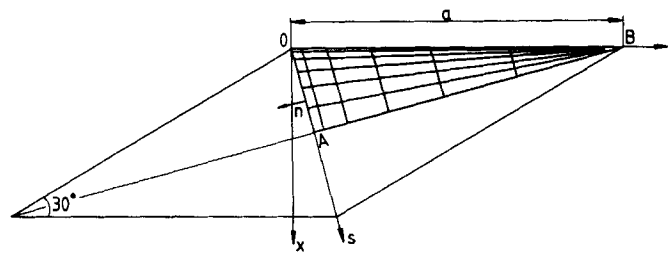

Figure 11. Rhombic plate (30°)

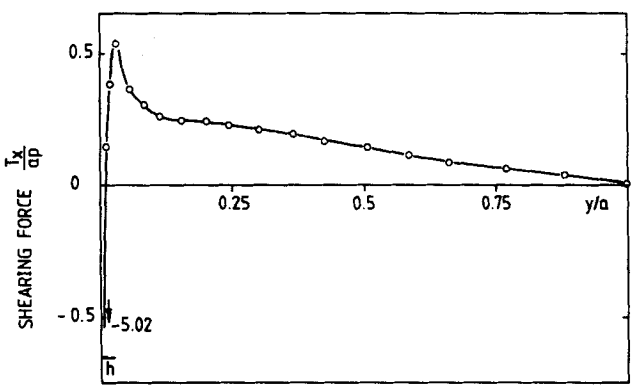

Figure 12. Shearing force distribution along OB

distributions in Figure 13 show good agreement with the Kirchhoff theory (solid curves), even quite near the corner. However, as anticipated, the moments approach zero within a boundary layer for the Reissner/Mindlin plate.

When Θ_s was restrained to zero along OB for the same model we obtained an overconstrained finite element model with oscillations in bounday shearing forces and a bad representation of the bending moments along OA, typically of a response prediction obtained with Kirchhoff theory based elements.

A transverse shearing force distribution (Figure 14) of somewhat different qualitative appearance is obtained in the analysis of a less skewed plate in Figure 15 ($\pi/\alpha = 18/7$, $\pi/\alpha = 18/11$). In

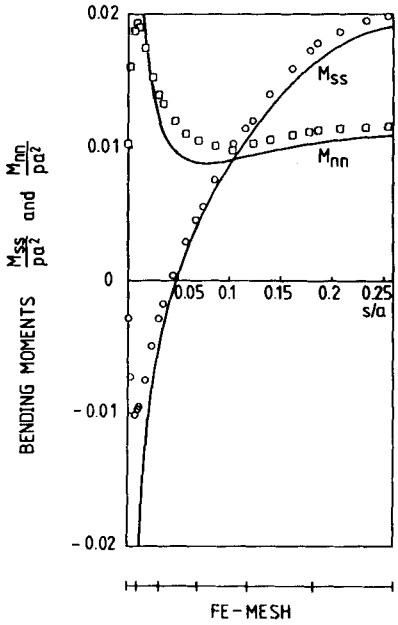

Figure 13. Bending moment distribution along OA

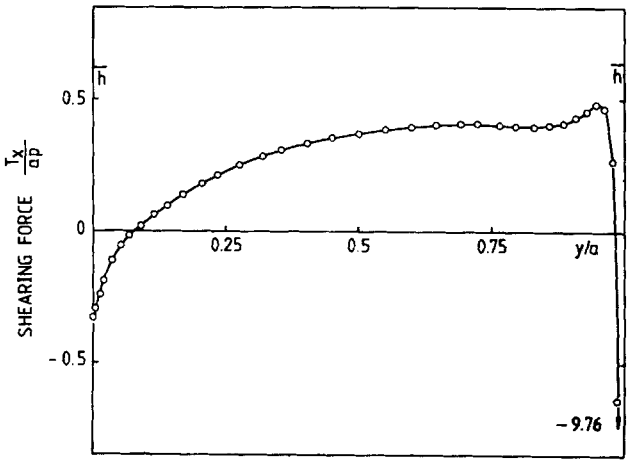

Figure 14. Shearing force distribution along OC

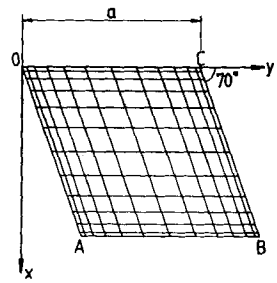

Figure 15. Rhombic plate (70°)

this case equation (58) predicts $\bar{T}_n(0) \sim h_0^{-15/11}$ in corner C and $\bar{T}_n(0) \sim h_0^{-3/7}$ in corner O and hence a boundary layer is expected in both corners. The formula (57) gives $0{\cdot}012a$ for the location of the zero passage near corner C. For corner O we obtain (as expected for acute angles) the less accurate value $0{\cdot}02a$.

6. CONCLUDING REMARKS

Substantial improvements in the description of the physical behaviour of plate structures may be obtained by using plate elements based on the Reissner/Mindlin theory. However, a reliable use demands proper specifications of the boundary conditions. For smooth edges (far from corners) it is shown in this paper that the transverse twist, the rotations and the stress resultants have boundary layers of different strengths and for some choices of boundary conditions (hard simply supported and soft clamped) there are no boundary layers for straight edges. For a corner with simply supported edges the behaviour of the boundary layer is studied along the edges. To satisfy the Reissner/Mindlin boundary condition of zero moment a boundary layer is set up near the corner that neutralizes the 'Kirchhoff singularity' and yields a complete solution for the moments and shear forces that is smooth although with high gradients. The theoretical predictions of the boundary layers are verified in numerical experiments with simply supported plates loaded by uniform pressure.

The results provide guidance in choosing meshes and proper boundary conditions in finite element analyses. For example, the need for fine meshes to resolve the edge zone behaviour may be anticipated from the expected strength of the different boundary layers. In an obtuse corner (soft simply supported edges), especially the inner part of the boundary layer puts great demands on the mesh resolution to capture the maximum bending moments. Valuable information about the physical behaviour near and on the boundary may be filtered out by an unfortunate choice of boundary conditions. Since the curvature of the boundary curve sometimes controls the boundary layer, care must be taken when modelling curved boundaries using plate bending elements with straight sides. When hard simply supported or soft clamped boundary conditions are chosen the boundary layers may be unintentionally suppressed, leading to an error that might not be negligible in a larger part of a moderately thick plate. Also, the removal of a Kirchhoff singularity presupposes a boundary layer. Since these two kinds of boundary conditions give rise to an unphysical behaviour they should be used with caution (see Reference 22). An important conclusion is that, in finite element analyses it is, provided the physical situation permits it, preferable to leave the rotation normal to the boundary free (soft conditions). Numerical experiments indicate that this usually prevents overconstraining in models of generally shaped

plates and is effective even if the purpose of the analysis is not primarily to resolve the boundary layers.

ACKNOWLEDGEMENTS

The authors would like to thank D. N. Arnold and I. Babuska for helpful dicussions and valuable criticism on this research.

APPENDIX

For the natural co-ordinate system (n, s) in Figure 2 we obtain the curvature of the boundary as $\dot{\varphi} = \partial\varphi/\partial s$, where φ also satisfies $\partial\varphi/\partial n = 0$. The following formulas are valid:[23]

$$\frac{\partial}{\partial n}\frac{\partial}{\partial s} - \frac{\partial}{\partial s}\frac{\partial}{\partial n} + \dot{\varphi}\frac{\partial}{\partial s} = 0 \tag{A1}$$

and

$$\nabla^2 = \frac{\partial^2}{\partial n^2} + \frac{\partial^2}{\partial s^2} + \dot{\varphi}\frac{\partial}{\partial n} \tag{A2}$$

The bending and twisting moments are expressed in terms of rotations by

$$\bar{M}_{nn} = \frac{\partial\Theta_n}{\partial n} + \nu\left(\frac{\partial\Theta_s}{\partial s} + \dot{\varphi}\Theta_n\right) \tag{A3}$$

$$\bar{M}_{ss} = \frac{\partial\Theta_n}{\partial s} + \dot{\varphi}\Theta_n + \nu\frac{\partial\Theta_n}{\partial n} \tag{A4}$$

and

$$\bar{M}_{ns} = \frac{1-\nu}{2}\left(\frac{\partial\Theta_s}{\partial n} + \frac{\partial\Theta_n}{\partial s} - \dot{\varphi}\Theta_s\right) \tag{A5}$$

The local transverse twist Ω is defined by

$$\Omega = \frac{1}{2}\left(\frac{\partial\Theta_s}{\partial n} - \frac{\partial\Theta_n}{\partial s} + \dot{\varphi}\Theta_s\right) \tag{A6}$$

The transverse shearing forces are given by

$$\bar{T}_n = \frac{6k(1-\nu)}{h^2}\left(\frac{\partial w}{\partial n} + \Theta_n\right) \tag{A7}$$

$$\bar{T}_s = \frac{6k(1-\nu)}{h^2}\left(\frac{\partial w}{\partial s} + \Theta_s\right) \tag{A8}$$

The equilibrium equations are

$$\frac{\partial\bar{M}_{nn}}{\partial n} + \frac{\partial\bar{M}_{ns}}{\partial s} + \dot{\varphi}(\bar{M}_{nn} - \bar{M}_{ss}) = \bar{T}_n \tag{A9}$$

$$\frac{\partial\bar{M}_{ns}}{\partial n} + \frac{\partial\bar{M}_{ss}}{\partial s} + 2\dot{\varphi}\bar{M}_{ns} = \bar{T}_s \tag{A10}$$

$$\frac{\partial\bar{T}_n}{\partial n} + \frac{\partial\bar{T}_s}{\partial s} + \dot{\varphi}\bar{T}_n = -f \tag{A11}$$

REFERENCES

1. K. J. Bathe, *Finite Element Procedures in Engineering Analysis*, Prentice-Hall, Englewood Cliffs, New Jersey, 1982.
2. T. J. R. Hughes and T. E. Tezduyar, 'Finite elements based upon Mindlin plate theory with particular reference to the four-node bilinear isoparametric element', *J. Appl. Mech. ASME*, **48,** 587–596 (1981).
3. K. J. Bathe and E. N. Dvorkin, 'A four node plate bending element based on Reissner/Mindlin plate theory and a mixed interpolation', *Int. j. numer. methods eng.*, **21,** 367–382 (1985).
4. K. J. Bathe and E. N. Dvorkin, 'A formulation of general shell elements—The use of mixed interpolation of tensorial component', *Int. j. numer. methods eng.*, **22,** 697–722 (1986).
5. E. Hinton and H. C. Huang, 'A family of quadrilateral Mindlin plate elements with substitute shear strain fields', *Comp. Struct.*, **23,** 409–431 (1986).
6. F. Brezzi, K. J. Bathe and M. Fortin, 'Mixed-interpolated elements for Reissner/Mindlin plates', *Int. j. numer. methods eng.*, **28,** 1787–1801 (1989).
7. K. J. Bathe, F. Brezzi and S. Cho, 'The MITC7 and MITC9 plate bending elements', *J. Comp. Struct.*, **32,** 797–814 (1989).
8. P. G. Ciarlet and P. Destuynder, 'Approximation of three-dimensional models by two-dimensional models in plate theory', in R. Glowinski *et al.* (eds.), *Energy Methods in Finite Element Analysis*, Wiley, New York, 1979, pp. 33–44.
9. S. P. Timoshenko and Woinowsky-Krieger, *Theory of Plates and Shells*, McGraw-Hill, New York, 1959.
10. K. J. Bathe and F. Brezzi, 'On the convergence of a four-node plate bending element based on Reissner/Mindlin plate theory and mixed interpolation', in J. R. Whitman (ed.), *Proc. MAFELAP Conference*, Brunel University, May 1984.
11. K. O. Friedrichs and R. F. Dressler, 'A boundary layer theory for elastic plates', *Commun. Pure Appl. Math.*, **14,** 1 (1961).
12. E. Reissner, 'On the theory of transverse bending of elastic plates', *Int. J. Solids Struct.*, **12,** 545–554 (1976).
13. E. Reissner, 'On the analysis of first and second-order shear deformation effects for isotropic elastic plates', *J. Appl. Mech. ASME*, **47,** 959–961 (1980).
14. D. N. Arnold and R. S. Falk, 'The boundary layer for the Reissner–Mindlin plate model', *SIAM J. Math. Anal.*, submitted.
15. D. N. Arnold and R. S. Falk, 'The boundary layer for the Reissner–Mindlin plate model: Soft simply supported, soft clamped and free plates', to appear.
16. E. Reissner, 'The effect of transverse shear deformation on the bending of elastic plates', *J. Appl. Mech. ASME*, **12,** A69 (1945).
17. R. D. Mindlin, 'Influence of rotary inertia and shear on flexural motions of isotropic elastic plates', *J. Appl. Mech. ASME*, **18,** 31–38 (1951).
18. R. E. O'Malley, *Introduction to Singular Perturbations*, Academic Press, New York, 1974.
19. T. Kant and E. Hinton, 'Mindlin plate analyses by segmentation method', *J. Eng. Mech. ASME*, **109,** 537–556 (1983).
20. M. L. Williams, 'Surface stress singularities resulting from various boundary conditions in angular corners of plates under bending', *Proc. First U.S. National Congress of Applied Mechanics*, 1951, pp. 325–329.
21. L. S. D. Morley, *Skew Plates and Structures*, Pergamon Press, Oxford, 1963.
22. I. Babuska and T. Scapolla, 'Benchmark computation and performance evaluation for a rhombic plate bending problem', *Int. j. numer. methods eng.*, **28,** 155–179 (1989).
23. B. M. Fraeijs de Veubeke, *A Course in Elasticity*, Springer-Verlag, Berlin, 1979.
24. K. J. Bathe and S. Bolourchi, 'A geometric and material nonlinear plate and shell element', *J. Comp. Struct.*, **11,** 23–48 (1980).